scientific reports

Check for updates

OPEN

Seasonal-to-interannual hydroclimatic variability in Afromontane environments during the late Early Pleistocene hominin occupations on the Southeastern Ethiopian Highlands

Giuseppe Briatico[1,2,3]✉, Gideon Hartman[2]✉, Tegenu Gossa[1,4], Asfawossen Asrat[5,6], Haregwin Hailu[7], Natnael Ketema[4], Bienvenido Martínez-Navarro[8,9,10], Elizabeth M. Niespolo[11,12,13], Paul R. Renne[12,13], Angesom Resom[12,14] & Erella Hovers[1,15,16,17]

Climate variability is a key factor influencing the distribution and adaptive response of mammalian species, including hominins. Here, we investigate seasonal and interannual hydroclimatic and environmental variability associated with the late Early Pleistocene hominin occupations on the Southeastern Ethiopian Highlands. We present stable carbon and oxygen isotope analyses of sequentially sampled tooth enamel from herbivores recovered from the archaeological contexts of Melka Wakena and Gadeb (2300–2400 m a.s.l.) and dated between 1.6 and ~1.0 Ma. Carbon isotope data indicate predominantly C_4 and mixed C_3–C_4 diets, consistent with mosaic vegetation as part of the Dry evergreen Afromontane Forest and grassland complex (DAF). Intra-tooth oxygen isotope profiles suggest seasonal variability and interannual fluctuations in water balance, reflecting changes in precipitation, evaporation, and local hydrology. Although the temporal resolution of individual tooth records precludes identification of specific climatic drivers, the isotopic data document recurring hydroclimatic variability within high-elevation environments characterized by broadly comparable ecological conditions. Herbivore diets show limited long-term change, suggesting sustained resource availability across seasons and over hundreds of thousands of years. These results indicate that the Ethiopian Highlands repeatedly supported mammalian communities and recurrent Acheulean hominin occupations during the late Early Pleistocene, providing sustained access to water and vegetation resources within an Afromontane environmental framework.

Reconstructing past ecosystems and their connections to climate is essential for understanding the expansions and contractions of Plio-Pleistocene hominin populations within Africa and beyond. Paleoenvironmental data

[1]Institute of Archaeology, The Hebrew University of Jerusalem, Jerusalem, Israel. [2]Department of Anthropology, University of Connecticut, Storrs, USA. [3]Dipartimento di Chimica "Giacomo Ciamician", University of Bologna, Bologna, Italy. [4]Department of History and Heritage Management, Arba Minch University, Arba Minch, Ethiopia. [5]Department of Geology and Geological Engineering, Botswana International University of Science and Technology, Palapye, Botswana. [6]School of Earth Sciences, Addis Ababa University, Addis Ababa, Ethiopia. [7]Laboratory Paleontology Evolution Paleoecosystems Paleoprimatology, UMR 7262 University of Poitiers and CNRS (PALEOVOPRIM), Poitiers, France. [8]Institut Català de Paleoecologia Humanai Evolució Social (IPHES-CERCA), Tarragona, Spain. [9]Departament d'Història i Història de l'Art, Universitat Rovira i Virgili, Tarragona, Spain. [10]ICREA, Barcelona, Spain. [11]Department of Geosciences, Princeton University, Princeton, USA. [12]Department of Earth and Planetary Science, University of California, Berkeley, USA. [13]Berkeley Geochronology Center, Berkeley, USA. [14]Department of Geology, Aksum University, Axum, Ethiopia. [15]Institute of Human Origins, Arizona State University, Tempe, USA. [16]ICArHEB, University of Algarve, Algarve, Portugal. [17]Minerva Center for the Study of Population Fragmentation, The Hebrew University of Jerusalem, Jerusalem, Israel. ✉email: giuseppe.briatico@unibo.it; gideon.hartman@uconn.edu

from northern[1], central[2,3], southern[4,5], and eastern Africa[6–16] emphasize the significance of heterogeneous habitats, microhabitats, and mosaic environments as key factors that shaped the geographic distribution of mammalian species[17–26].

On the Ethiopian highlands, at elevations of ~2000 m above sea level (m a.s.l.) and higher, palynological studies from Gadeb and Melka Kunture have documented Plio-Pleistocene environmental changes, revealing variable proportions of grasslands, wooded and forested vegetation within the Dry evergreen Afromontane Forest and grassland complex (DAF)[27,28]. Temporal changes in pollen abundance are attributed to orbitally forced climatic events[28]. Today, the DAF vegetation thrives primarily on the Ethiopian highlands at elevations above 1800 m a.s.l., such as in the Shashemene Forest (2010 m a.s.l.) and the Bale Mountains (4377 m a.s.l.)[27,28]. In contrast, plain areas within this elevation range are largely modified by human activity, mainly for agriculture and grazing[27,29,30].

The modern climate of the Ethiopian highlands is shaped by the Indian Monsoon and the movement of air masses linked to the Intertropical Convergence Zone (ITCZ), producing a bimodal seasonal rainfall regime[31,32]. During the dry season (*Bega*, from October to December/January), the region is influenced by a dry northeastern continental air mass. The ITCZ brings rainfall to the southern and southwestern areas between February/March and May (short rainy season, *Belg*). From June to September, the southwestern airstream extends over the Ethiopian highlands, generating the main rainy season (*Kiremt*)[32,33]. The timing and movement of the ITCZ vary annually, contributing to pronounced interannual variability in rainfall across Ethiopia. These patterns are further modulated by the El Niño-Southern Oscillation (ENSO), with El Niño typically associated with reduced *Kiremt* rainfall during its warm phase, and La Niña linked to its cool phase and potentially enhanced rainfall[34–41].

Here, we employ stable carbon and oxygen isotope analysis of 312 sequential enamel samples from 14 teeth belonging to three mammalian families: Hippopotamidae, Bovidae, and Equidae (Table 1). The teeth were recovered from stratigraphically secure, dated sedimentary sequences at the Melka Wakena (MW) and Gadeb (GB) archaeological site-complex, situated in the Gadeb Plain (as defined in Hovers et al.[42]) on the Southeastern Ethiopian Highlands between 2300 and 2400 m a.s.l. (Fig. 1) (see Supplementary Text A for dating, stratigraphy, and archaeological evidence)[42–47]. The isotopic data enable reconstruction of hydroclimatic and local environmental conditions on a multi-seasonal scale between 1.6 and ~1.0 million years (Ma) ago. We compare our dataset with the published isotopic record from Melka Kunture (MK)[15,16], located on the western shoulder of the Main Ethiopian Rift at 2000–2200 m a.s.l (Fig. 1). By placing this information in a broader geographic framework, we aim to document the ecological dynamics that hominin groups associated with the Acheulean technocomplex (e.g., *Homo erectus sensu lato*), experienced during the late Early Pleistocene on the Ethiopian highlands.

Results

The $\delta^{13}C$ and $\delta^{18}O$ isotope measurements of enamel bioapatite are summarized in Table S1, where the data are grouped by faunal family and presented chronologically from the oldest to the youngest specimens, including the median for each isotopic profile. Figure 2 illustrates the overall isotopic ranges, whereas Fig. 3 displays the intra-tooth profiles of the analyzed taxa.

As shown in Fig. 2A–F, $\delta^{13}C$ and $\delta^{18}O$ values of six hippo isotopic profiles ($n = 230$) range from −3.6‰ to +2.09‰ (mean = −0.08‰) and from −7.9‰ to −0.4‰ (mean = −5.6‰), respectively. The $\delta^{13}C$ values of five bovid teeth ($n = 40$) vary from −0.4‰ to +5.4‰ (mean = +3‰), whereas $\delta^{18}O$ values range from −8.2‰ to −0.5‰ (mean = −4.4‰) (Fig. 2G–K). The three equid isotopic profiles ($n = 42$) show $\delta^{13}C$ values ranging from −2.9‰ to +1.9‰ (mean = −0.5‰) and $\delta^{18}O$ values that range from −5.9‰ to −0.9‰ (mean = −4.3‰) (Fig. 2L–N). Only three isotopic values (a single $\delta^{18}O$ value in Fig. 2F; two $\delta^{13}C$ values in Fig. 2G) deviate substantially from the overall data distribution and are therefore considered outliers.

	Fauna ID	Age (Ma)	Element	Family	Tribe	Genus	Species
A	**MW2-L3-B787**	**1.6**	**Left lower canine fragment**	**Hippopotamidae**	**Hippopotamini**	***Hippopotamus***	***Hippoptamus gorgops***
B	MW n.d.	1.6	Canine	Hippopotamidae	Hippopotamini	*Hippopotamus*	*Hippoptamus gorgops*
C	MW2-L1&L2	1.45–1.34	Upper canine	Hippopotamidae	Hippopotamini	*Hippopotamus*	*Hippoptamus gorgops*
D	G8E-G64	~1.0	Lower left canine	Hippopotamidae	Hippopotamini	*Hippopotamus*	*Hippoptamus* cf. *gorgops*
E	G8D-G328-D1	~1.0	Lower right canine	Hippopotamidae	Hippopotamini	*Hippopotamus*	*Hippoptamus* cf. *gorgops*
F	G8D-G133-D2	~1.0	Lower left canine	Hippopotamidae	Hippopotamini	*Hippopotamus*	*Hippoptamus* cf. *gorgops*
G	MW2-L3-B695	1.6	Left lower m^3	Bovidae	-	–	–
H	MW2-L3-B233	1.6	Right lower m^2	Bovidae	-	–	–
I	MW2-L3-B579	1.6	Right upper M^3	Bovidae	Tragelaphini	–	–
J	MW3	1.6	Right upper M^3	Bovidae	Aepycerotini	*Aepyceros*	–
K	G2E-G507-K1	~1.45	Right upper M^2	Bovidae	Alcelaphini	–	–
L	MW8	1.6	Left upper M^3	Equidae	Equini	*Equus*	–
M	G2E-G496-L1	~1.45	Incisor	Equidae	Equini	*Equus*	–
N	G8-G49	~1.0	Lower left m^2	Equidae	Equini	*Equus*	–

Table 1. Information on the faunal remains from Melka Wakena and Gadeb used in this study.

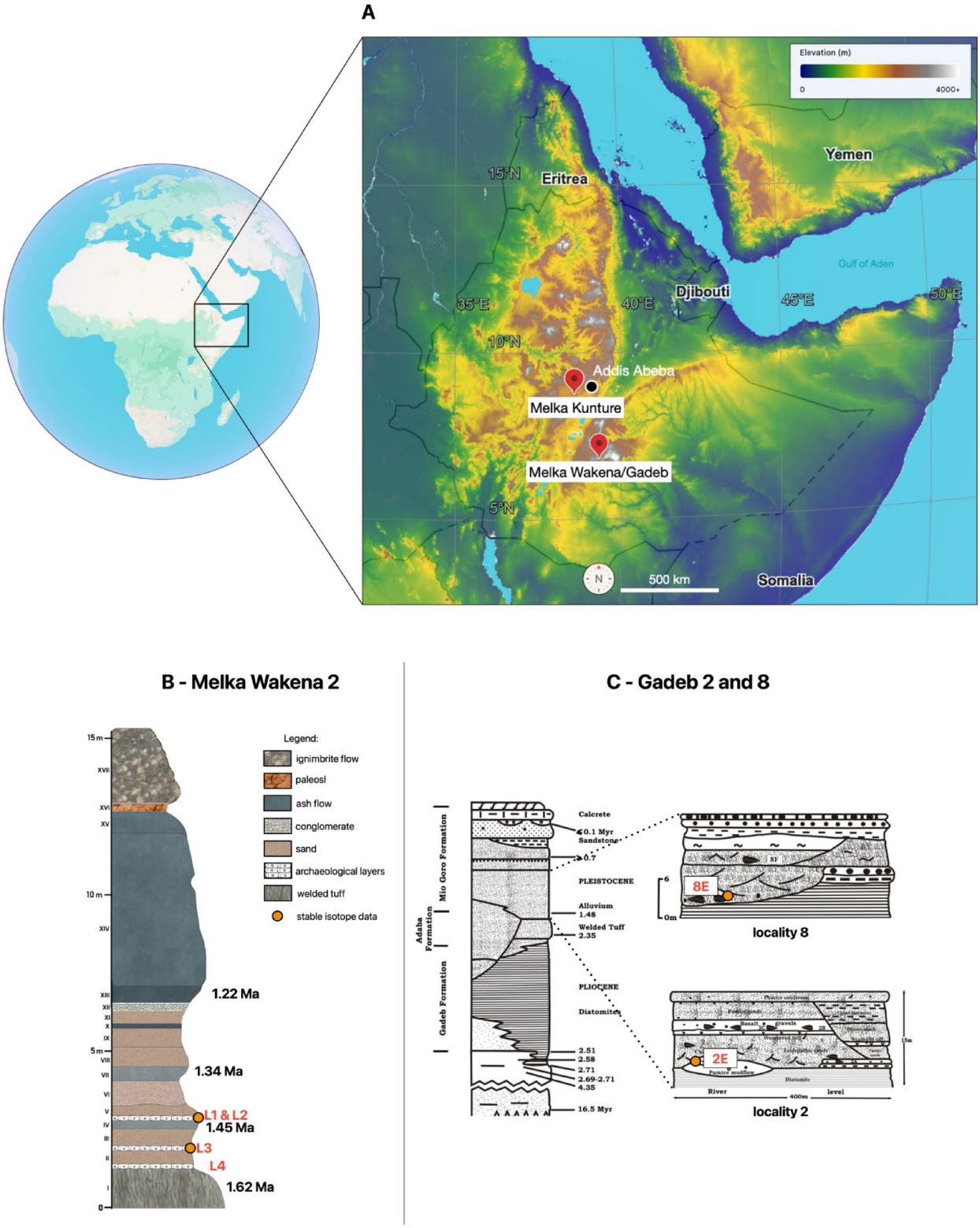

Fig. 1. Archaeological and paleontological sites. Top panel: (**A**) Context of the study region in eastern Africa and location map of the Melka Wakena and Gadeb site-complexes on the Southeastern Ethiopian Highlands, including the location of Melka Kunture (MK) and Addis Ababa (Google Earth Pro 7.3.6); Bottom panel: (**B**) Stratigraphic section of Melka Wakena 2, showing the archaeological layers (red) and dated tephra deposits (dates rounded to the nearest decimal point, after Hovers et al.[42]). Samples from localities MW3 and MW8 (Table S1) are stratigraphically coeval with MW2-L3; (**C**) Stratigraphy of Gadeb, including stratigraphic logs of localities 2 and 8 discussed in the text (modified after de la Torre[47]. For additional details, readers are referred to Supplementary Text A.

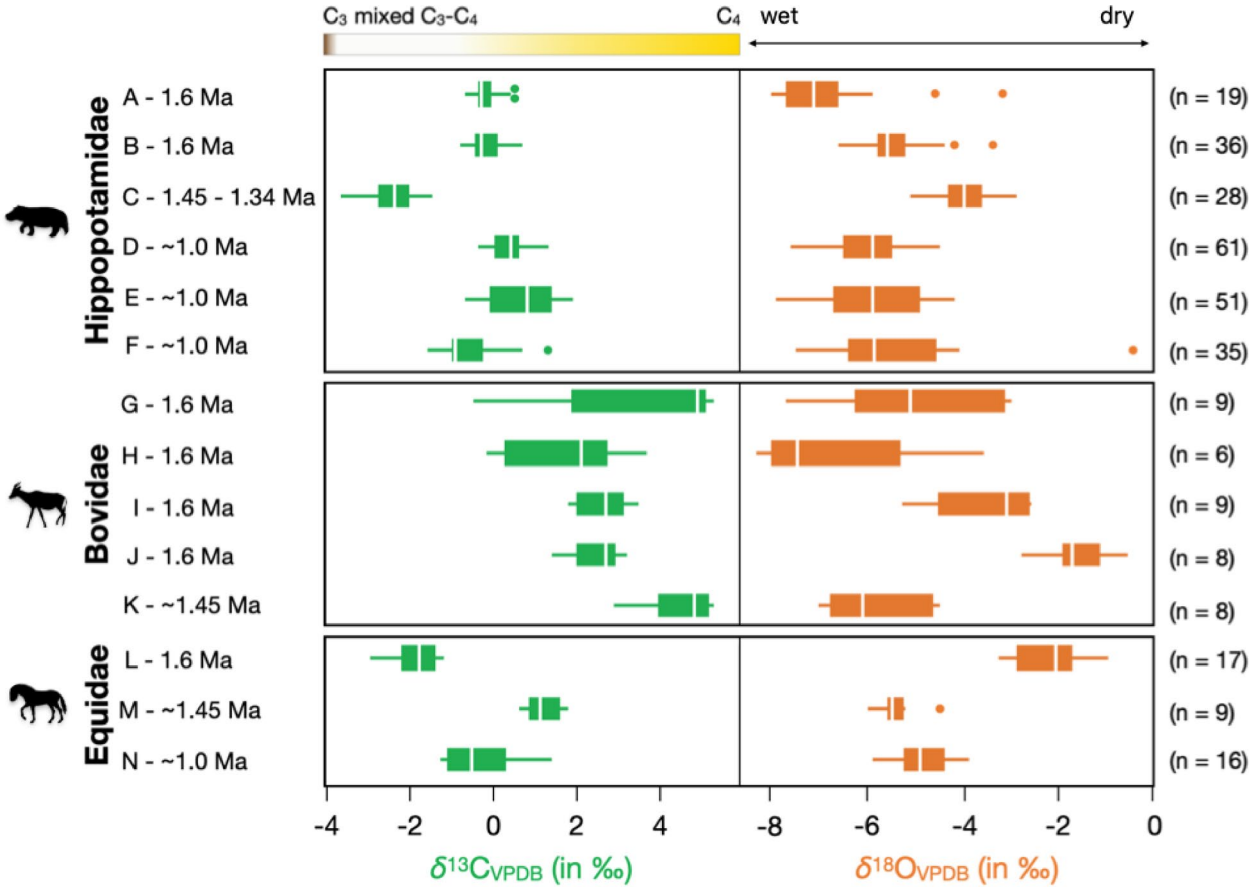

Fig. 2. Solid box plots of $\delta^{13}C$ (green) and $\delta^{18}O$ (orange) intra-tooth values for (**A**–**F**) hippos, (**G**–**K**) bovids, and (**L**–**N**) equids from MW and GB. The isotopic data are grouped by faunal family, with each group arranged chronologically from the oldest (1.6 Ma) to the youngest (~ 1.0 Ma). Each box plot represents a single tooth. Specimen labels (**A**–**N**) correspond to the individual specimens listed in Table 1 and Table S1 (Excel file). The box represents the interquartile range, the vertical white line indicates the median, the whiskers extend to the most extreme non-outlier values, and the points correspond to outliers. Animal silhouettes are from https://www.phylopic.org.

Normal quantile plots and Shapiro-Wilk tests indicate non-normal distributions of $\delta^{13}C$ and $\delta^{18}O$ values for hippos ($p = 0.0001$ and $p = 0.0038$) and equids ($p = 0.0069$ and $p = 0.0022$) (Supplementary Fig. 2A and C). Bovids show non-normal $\delta^{13}C$ values ($p = 0.0262$) but normally distributed $\delta^{18}O$ values ($p = 0.1878$) (Supplementary Fig. 2B). Levene's tests reveal unequal variances for both $\delta^{13}C$ and $\delta^{18}O$ values in hippos ($p = 0.0001$), and unequal $\delta^{13}C$ but equal $\delta^{18}O$ variances in bovids ($p = 0.0033$ and $p = 0.0867$) and equids ($p = 0.0414$ and $p = 0.1033$). Wilcox/Kruskal-Wallis tests confirm that all taxa differ significantly in both $\delta^{13}C$ and $\delta^{18}O$ rank ($p = 0.0001$).

Four of the six hippo specimens show significant cross-correlation between $\delta^{13}C$ and $\delta^{18}O$ profiles ($R > 0.5$) (Supplementary Fig. 3A, D, E and F), while two specimens exhibit no significant cross-correlation ($R < 0.5$) (Supplementary Fig. 3B and C). Among bovids, two specimens show significant cross-correlation (Supplementary Fig. 3G and H), whereas the remaining three do not (Supplementary Fig. 3I, J and K). For equids, two specimens also show significant cross-correlation (Supplementary Fig. 3L and M), and one shows no significant correlation (Supplementary Fig. 3N).

Discussion

Seasonal-to-interannual variability in $\delta^{13}C$ and $\delta^{18}O$ isotopic profiles

Stable carbon and oxygen isotope analyses of sequentially sampled herbivore tooth enamel document multi-seasonal variations in diet, drinking water, and local hydroclimatic and environmental conditions throughout the interval of enamel mineralization[48–55]. In this context, seasonality refers to the cyclical fluctuations in rainfall throughout the year that influence ecosystem composition and resource availability.

Stable isotope analysis of hippos' ever-growing canines and incisors (often referred to as tusks) provides high-resolution isotopic records across tooth enamel formation[56–59]. Deciduous tusks erupt at birth and are shed at ~ 14 months, after which permanent open-rooted canines and incisors grow continuously throughout life[60]. Interpreting temporal patterns along the tooth growth axis requires assumptions about enamel growth rates, which remain incompletely constrained and show substantial inter-individual variability. Passey et al.[61] measured growth rates of 29 and 13 mm/year in the lower canines of two female common hippos of different

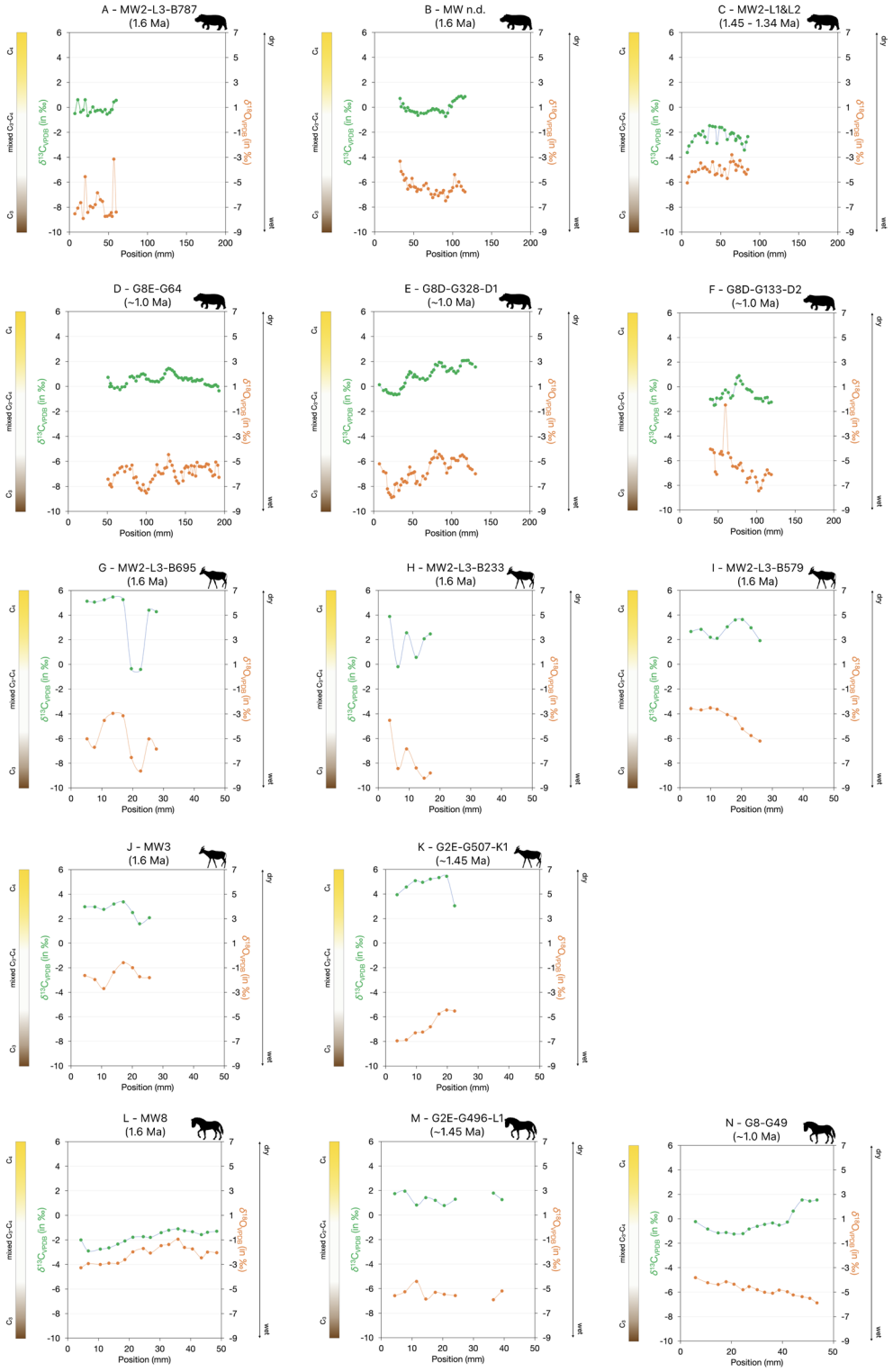

Fig. 3. Intra-tooth variation in stable carbon ($\delta^{13}C$, green circle) and oxygen ($\delta^{18}O$, orange circle) isotope ratios measured along the fossil teeth of hippos (**A**–**F**), bovids (**G**–**K**), and equids (**L**–**N**) from MW and GB. The isotopic data are grouped by faunal family, with each group arranged chronologically from the oldest (1.6 Ma) to the youngest (~ 1.0 Ma). Specimen labels (**A**–**N**) correspond to the individual specimens listed in Table 1 and Table S1 (Excel file). The time of tooth mineralization proceeds on the x-axis from left (older enamel–top of the tooth) to right (younger enamel – bottom of the tooth). Position on the x-axis refers to the location of each sample along the tooth growth axis (in millimeters). The samples collected from the teeth are scaled at 200 mm for hippos and 50 mm for bovids and equids. Animal silhouettes are from https://www.phylopic.org.

ages, while Souron et al.[56] reported rates of 31–39 mm/year in modern females and noted less distinct isotopic cyclicity in fossil specimens, consistent with slower or more variable growth (20–30 mm/year)[56]. Uno et al.[62] documented additional variability related to sex and tooth position, with growth rates ranging from 19 to > 70 mm/year[62]. Because most published growth rates derive from modern, known-age individuals[56,61,62], their direct application to Pleistocene hippos assumes constancy in life history traits that may not hold under past environmental or selective pressures. While destructive approaches such as histological thin sections or die-saw dicing could potentially refine growth estimates[55,61–67], their application is limited in paleontological contexts.

In our dataset, two hippo canines from GB (Fig. 3D and E), for which a larger sample size is available ($n = 61$ and 51 samples, respectively), exhibit quasi-cyclical $\delta^{13}C$ and $\delta^{18}O$ variation patterns. Four of the six hippo intra-tooth profiles show $\delta^{13}C$ variability within the C_4 range (Fig. 3A, B, D, and E), indicating consumption of grasses with differing C_4 photosynthetic pathways[68–71]. By contrast, two specimens (Fig. 3C and F) display lower $\delta^{13}C$ values consistent with mixed C_3–C_4 diets that incorporate C_3 vegetation such as cool-season grasses, browse, and aquatic plants[14–16,72].

As for the $\delta^{18}O$ values, the specimen shown in Fig. 3E records a positive interannual shift of approximately 5 years, based on growth rates of ~ 30 mm/year in Pleistocene hippos[56]. This trend is interpreted as reflecting increased evaporative water loss under relatively low rainfall, resulting in negative water balance and declining water levels during dry phases (see $\delta^{18}O$ min-max values and seasonal cycles in Supplementary Fig. 4B). In contrast, negative interannual shifts in other isotopic profiles recorded in Fig. 3B and F suggest water bodies under positive water balance, where high rainfall and low evaporation cause rising water levels that occur during wet phases (Supplementary Fig. 4A and C).

Comparable patterns are observed in published modern and fossil hippo isotopic records[56] (Supplementary Fig. 5), supporting a hydrological interpretation for these variations. In particular, the modern hippo specimen is from the area of Sarh in southern Chad[56], where seasonal rainfall variability is influenced by ENSO phases[73,74]. Based on this, we speculate that the interannual positive and negative trends recorded in our hippo isotopic profiles resemble the modern records of ENSO variability across the Horn of Africa[33–36], i.e., El Niño-like episodes corresponding to drier conditions, and La Niña-like episodes to wetter conditions. Further statistical and modeling analysis should be conducted to test this hypothesis, which we currently state with parsimony.

Cross-correlation analysis between intra-tooth $\delta^{13}C$ and $\delta^{18}O$ profiles clarifies the timing of ecological responses to hydroclimatic forcing. Some hippo individuals show strong positive correlations at zero lag (Supplementary Fig. 3E), indicating synchronous responses of water sources and vegetation to seasonal rainfall. In contrast, other individuals exhibit significant correlations at non-zero lags (Supplementary Fig. 3F), suggesting delayed dietary responses relative to hydrological inputs.

Among terrestrial herbivores, serially sampled bovid specimens (Fig. 3G–K) exhibit moderate intra-individual variability in both $\delta^{13}C$ and $\delta^{18}O$ values. Assuming published tooth growth rates of ~ 30–40 mm/year[75] for comparable taxa, one specimen (Fig. 3I) shows isotopic cyclicity that could be consistent with seasonal-scale variability, further supported by significant cross-correlation results.

Two equid specimens (Fig. 3L and N) record mixed C_3–C_4 diets with modest directional shifts in $\delta^{13}C$, whereas the equid profile in Fig. 3M indicates relatively stable C_4 grazing. In both bovids and equids, intra-tooth $\delta^{18}O$ variability likely reflects a combination of seasonal climate signals, physiological differences, drinking behavior, and potential mobility rather than local climate alone [56,57,74–78]. These interpretations are necessarily constrained by several limitations of the dataset. First, specimen availability is restricted by the archaeological nature of the assemblage, which limits both the number of individuals and the taxonomic resolution of several specimens. In particular, two bovid teeth cannot be identified beyond the family level, preventing confident assignment to specific feeding guilds or drinking strategies. Second, the relatively small number of individuals analyzed restricts the possibility of evaluating population-level ecological patterns, which is a common issue in the literature[1,8–10,56–58]. For these reasons, the interpretations presented here are framed conservatively and focus primarily on broad ecological trends rather than taxon-specific dietary or behavioral reconstructions.

Overall, the intra-tooth isotopic data from MW and GB indicate seasonal-to-interannual hydroclimatic variability within high-elevation Afromontane environments characterized by broadly similar ecological conditions across the sampled intervals. Frequent but variable coupling between $\delta^{13}C$ and $\delta^{18}O$ signals suggests that climatic fluctuations were propagated through local hydrological and vegetation systems, with no clear evidence for sustained changes in the analyzed herbivore diets within the limits of the available dataset.

Paleoecological inference

The dominance of C_4 isotopic signals in our dataset is consistent with expectations for elevations of MW and GB (2300–2400 m a.s.l.)[29]. In modern eastern Africa, C_4 grasses are most abundant below 2000 m, while C_3 grasses dominate above 3000 m[79], although exceptions are documented[80]. The mixed isotopic signals observed in our dataset, therefore, reflect the ecological heterogeneity expected at intermediate elevations rather than anomalous vegetation structure[16].

Our results support the preliminary interpretation of the late Early Pleistocene faunal assemblages from MW and GB (Supplementary Text A). When Acheulean-making hominins occupied the Gadeb Plain, the local environment predominantly consisted of montane grasslands dominated by C_4 grasses, interspersed with C_3 vegetation, shrubs, and aquatic habitats[42,81]. Studies of modern African ecosystems demonstrate that grazers commonly dominate herbivore assemblages even in landscapes with substantial woody cover[82,83]. Accordingly, the abundance of grazers at MW and GB should not be interpreted as evidence for extensive open grasslands alone, and caution is warranted against simplistic vegetation reconstructions based solely on taxonomic composition[42,82–84].

Although no pollen or phytolith data are currently available from the archaeological horizons of MW and GB discussed here[27,42], the enamel carbon isotope data provide evidence of animal feeding preferences and

associated habitats and, by extension, local environmental conditions during hominin occupations between 1.6 and ~1.0 Ma.

Because MW and GB share similar altitudinal and regional climatic settings with MK, we compared $\delta^{13}C$ and $\delta^{18}O$ values across these sites (Supplementary Text C; Supplementary Figs. 6–8; Supplementary Table 1). All three sites exhibit broadly overlapping isotopic ranges (Fig. 4A1–2), indicating comparable ecological conditions dominated by C_4 and mixed C_3–C_4 vegetation. This consistency suggests that broadly comparable Afromontane environmental conditions characterized the sampled high-elevation Ethiopian sites during the investigated intervals. We observe substantial overlap in $\delta^{18}O$ values among the three sites, and a possible positive trend in minimum $\delta^{18}O$ values between 1.6 and ~1.4 Ma (Fig. 5). This pattern is based on a limited number of measurements and is characterized by high variability and should be interpreted with caution. Rather than indicating a clear or systematic climatic shift, the data may reflect short-lived or local hydroclimatic fluctuations within the constraints of sparse sampling.

Notably, niche modelling of the 1.6–1.4 Ma Ethiopian wolf (*Canis simensis*) from MW[85] generated Habitat Suitability Index (HSI) maps that are broadly consistent with the $\delta^{18}O$ data. The model suggests higher HSI values at 1.6 Ma, associated with cooler conditions and a wider potential geographic range, and lower HSI values at 1.4 Ma, corresponding to warmer conditions and a reduced potential distribution[85]. We emphasize that links between the isotopic signal and modeled habitat suitability would require additional, higher-resolution datasets for robust evaluation.

We compared the median $\delta^{13}C$ and $\delta^{18}O$ values (Table S4) from MW, GB, and MK (high-elevation sites > 2000 m a.s.l.) with those from equivalent taxa at lower-elevation sites (≤ 1500 m a.s.l.) in the East African Rift System, including Oldupai Gorge, Lake Turkana Basin, and Busidima Formation. As noted in Briatico et al.[15], elevation does not appear to determine animal feeding behaviour in selecting vegetation, which remains dominated by C_4 resources across a wide altitudinal range. In contrast, high-elevation sites consistently yield lower $\delta^{18}O$ values than low-elevation sites, reflecting the isotopic altitude effect[86–88] and predictably indicating cooler conditions in the Ethiopian highlands (Fig. 4B1–2)[15]. In particular, hippos depend on submersion in stable water bodies for thermoregulation, in the absence of sweat glands[89], and are not a seasonally migratory species. Thus, hippo isotopic signals primarily reflect local hydrology and water bodies rather than long-distance movement. For bovids and equids, however, seasonal altitudinal movements cannot be excluded based on carbon and oxygen isotope data alone.

The persistent, albeit intermittent, archaeological, paleontological, and anthropological evidence recorded in the Early Pleistocene multi-layered deposits of the Ethiopian highlands[27–42,90–97] indicates that these environments repeatedly supported mammalian species, including *Homo erectus sensu lato* populations over extended periods. Rather than representing environmentally constrained settings, the Ethiopian highlands appear to have provided recurrent access to water and vegetation resources within the Afromontane environmental framework. Taken together, our results indicate that late Early Pleistocene high-elevation ecosystems were characterized by recurrent hydroclimatic variability within broadly comparable Afromontane environmental conditions, circumstances that may have promoted long-term hominin persistence. Distinct from the lowland Rift System, such environments may serve as informative analogues for the ecological settings faced by hominins during their dispersal out of Africa.

Methods

Stable isotope analysis

A total of 312 enamel samples were collected from 14 fossil teeth (Supplementary Fig. 1) excavated at various archaeological sites within the MW and GB areas (MW2, MW3, MW8; GB2, GB8), dated between 1.6 and ~1.0 Ma (Fig. 1). The fossil specimens include Hippopotamidae ($n = 230$ enamel samples), Bovidae ($n = 40$), and Equidae ($n = 42$) (Table S1). The specimens were purposely selected for intra-tooth sequential sampling in October/November 2023 at the Ethiopian Heritage Authority (EHA) facilities in Addis Ababa (Ethiopia), with the approval of EHA curators. Each sample lab code corresponds to the site abbreviation (MW = Melka Wakena; GB = Gadeb), followed by a progressive sample number (e.g., MW 1, MW 2; or GB 1, GB 2). First, the tooth surface was inspected to select the best sampling location. This area was systematically cleaned with a diamond drill bit (> 2.0 mm) to remove any extraneous material. Then, several enamel samples were taken with a diamond-tipped drill (< 2.0 mm) along the entire length of the tooth[56] (~2–2.5 mm intervals) to obtain 12–15 mg of enamel powder per sample, allowing for potential material loss during subsequent laboratory procedures. After collection and export, pretreatment was conducted at the Stable Isotope Preparation Lab, Department of Anthropology of the University of Connecticut (UConn) (Storrs, Connecticut, U.S.A.), following the protocol by Balasse et al.[98]. The powdered enamel samples were treated with 0.1 M acetic acid (CH_3COOH) for 4 h at room temperature to remove exogenous carbonate. The remaining samples were rinsed once or twice with MilliQ® water (Millipore) until the solution reached neutrality; then, the reaction tubes were placed in a desiccating oven to dry overnight at 50 °C. Weighed samples (1 mg) were sent for carbon and oxygen isotope analysis at the Yale Analytical and Stable Isotope Center (YASIC) of Yale University (New Haven, Connecticut, U.S.A.), using an automated carbonate preparation device (Kiel-IV) coupled to an isotope ratio mass spectrometer (Thermo MAT 253). Isotope measurements were calibrated using repeated analysis of three in-house and two international standards (NBS-19 and NBS-18). The analytical precision is ± 0.1‰ for $\delta^{18}O$ and ± 0.08‰ for $\delta^{13}C$ (1 σ). Carbon and oxygen isotope compositions are reported in standard δ-notation relative to the Vienna Pee Dee Belemnite (VPDB) standard. Details regarding the isotopic signal interpretation are provided in Supplementary Text B.

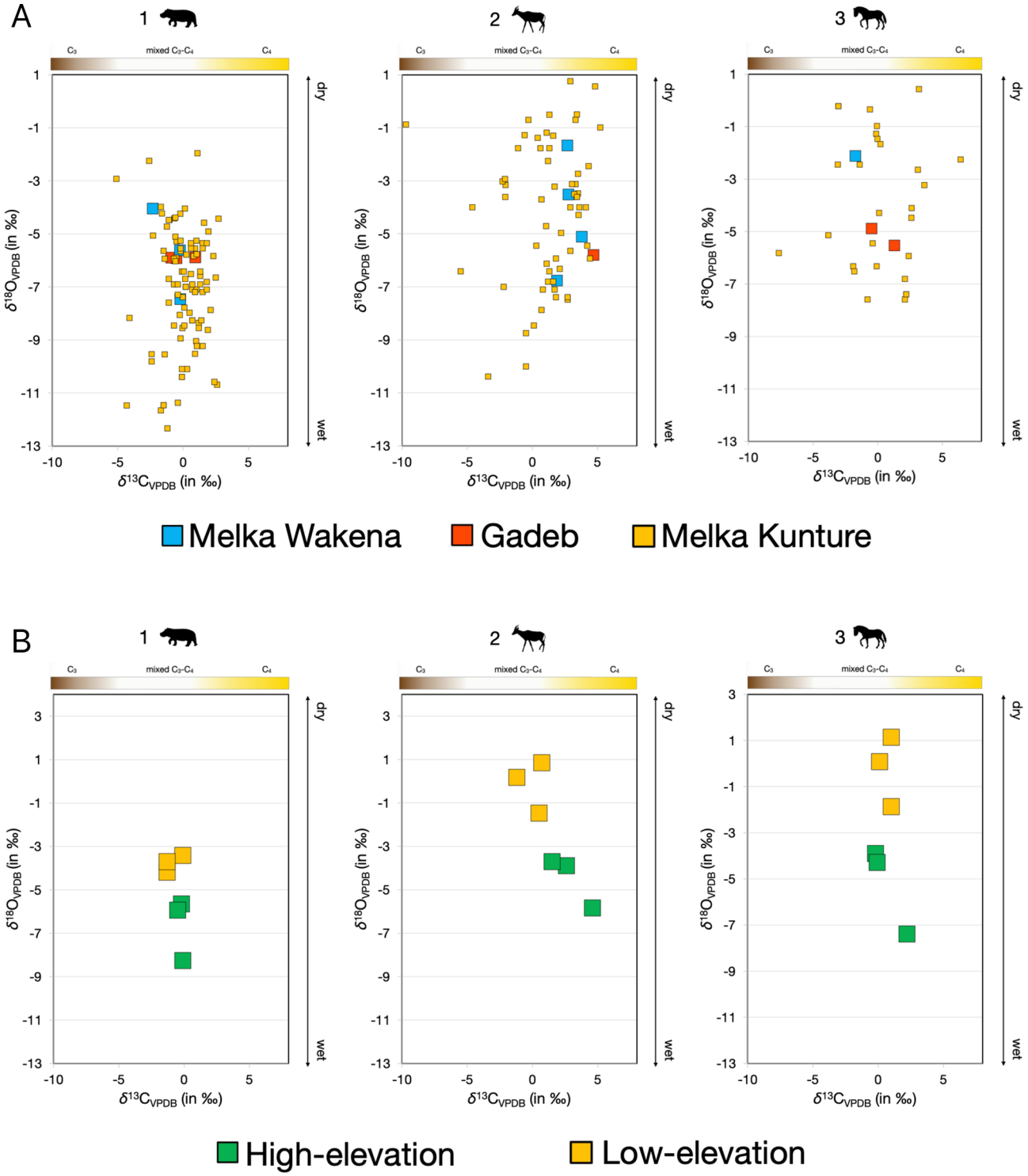

Fig. 4. Scatter plots of $\delta^{13}C$ and $\delta^{18}O$ values (**A**) for (1) hippos, (2) bovids and (3) equids from MW, GB and MK; median $\delta^{13}C$ and $\delta^{18}O$ values (**B**) of the same taxa from high- (> 2000 m a.s.l.; MW, GB and MK) and low-elevation (≤ 1500 m a.s.l.; Oldupai Gorge, Lake Turkana Basin and Busidima Formation) eastern African sites. The isotopic data utilized for the graphs are provided in Tables S2 and S4. Animal silhouettes are from https://www.phylopic.org.

Statistics and cross-correlation analysis

All statistical analyses were conducted using JMP Pro 18 (version 18.2.0; licensed by the Hebrew University of Jerusalem), with a significant threshold of $p = 0.05$. The $\delta^{13}C$ and $\delta^{18}O$ values were analyzed by faunal family to account for taxon-specific ecological variability. Normal quantile plots and the Shapiro-Wilk test were used to

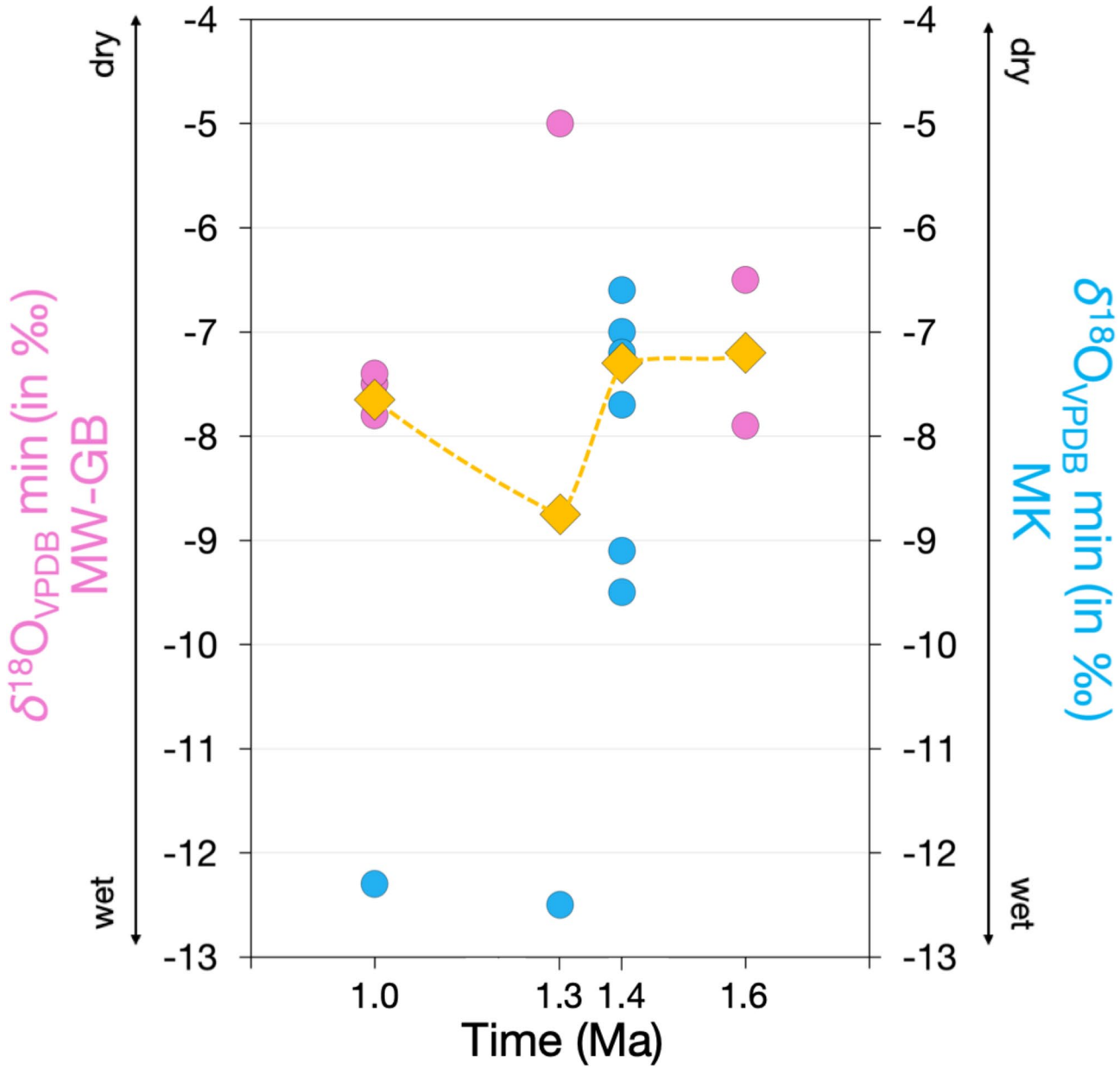

Fig. 5. Scatter plots of $\delta^{18}O$ min values of hippo intra-tooth profiles from MW-GB (pink circle) and MK (blue circle) plotted against chronology. Between 1.6 and ~ 1.4 Ma, positive stable oxygen isotopic values appear to indicate drier climatic conditions compared to those recorded at ~ 1.3 and 1.0 Ma. Median values are in yellow, with trends marked by a yellow dashed line.

assess the assumption of normality. In this framework, the null hypothesis (H_0) states that the data are drawn from a normally distributed population, whereas the alternative hypothesis (H_1) indicates a non-normal distribution. Because group sizes are unequal, homogeneity of variance was evaluated using Levene's test, which assesses whether the absolute deviation from group means differ among groups. Here, H_0 assumes equal variances across taxonomic groups, while H_1 indicates unequal variances.

When the assumptions of normality and/or homoscedasticity were violated, non-parametric tests were applied. Differences in $\delta^{13}C$ and $\delta^{18}O$ values among more than two independent taxonomic groups were evaluated using the Kruskal–Wallis test, which compares rank distributions across groups. When the Kruskal–Wallis test indicated a significant overall effect, pairwise post-hoc comparisons were conducted using Wilcoxon rank-sum tests. For comparisons involving two independent groups only, Wilcoxon rank-sum tests were used directly. The same analytical framework was applied when comparing $\delta^{13}C$ and $\delta^{18}O$ values across taxa and archaeological sites (MW, GB, and MK; Supplementary Text C). The degree of correlation between the $\delta^{13}C$ and $\delta^{18}O$ values within individual intra-tooth isotopic profiles (Supplementary Fig. 3) was assessed using cross-correlation analysis implemented with the "*ccf*" function in RStudio (version 2023.06.0 + 421). This analysis was used to evaluate whether changes in $\delta^{18}O$ values could temporally precede or coincide with shifts in $\delta^{13}C$

values. Cross-correlation coefficients (R) ≥ 0.5 were interpreted as strong correlations, whereas values < 0.5 were considered weak.

Data availability

The data generated and analyzed during the study are available in this published article and its Supplementary Information files. Original fossils are housed at the EHA facilities in Addis Ababa; the remaining enamel powder samples are stored at the Stable Isotope Preparation Lab (UConn, Department of Anthropology).

Code availability

No code has been created for this study.

Received: 13 November 2025; Accepted: 29 June 2026
Published online: 02 July 2026

References

1. Ramírez-Pedraza, I. et al. Arid, mosaic environments during the Plio-Pleistocene transition and early hominin dispersals in northern Africa. *Nat. Commun.* **15**, 8393 (2024).
2. Zazzo, A. et al. Herbivore paleodiet and paleoenvironmental changes in Chad during the Pliocene using stable isotope ratios of tooth enamel carbonate. *Paleobiology* **26**, 294–309 (2000).
3. Lee-Thorp, J. et al. Isotopic evidence for an early shift to C_4 resources by Pliocene hominins in Chad. *Proc. Natl Acad. Sci. USA* **109**, 20369–20372 (2012).
4. Lee-Thorp, J. A., Sponheimer, M. & Luyt, J. Tracking changing environments using stable carbon isotopes in fossil tooth enamel: an example from the South African hominin sites. *J. Hum. Evol.* **53**, 595–601 (2007).
5. Lehmann, S. B. et al. Stable isotopic composition of fossil mammal teeth and environmental change in southwestern South Africa during the Pliocene and Pleistocene. *Palaeogeogr Palaeoclimatol Palaeoecol*. **457**, 396–408 (2016).
6. Bedaso, Z., Wynn, J. G., Alemseged, Z. & Geraads, D. Paleoenvironmental reconstruction of the Asbole fauna (Busidima Formation, Afar, Ethiopia). *Geobios* **43**, 165–177 (2010).
7. van der Merwe, N. J. Isotopic ecology of fossil fauna from Olduvai Gorge at ca 1.8 Ma, compared with modern fauna. *S Afr. J. Sci.* **109**, 11–12 (2013).
8. Ascari, S. H., Njau, J. K., Sauer, P. E., Polly, P. D. & Peng, Y. Fossil herbivores and crocodiles as paleoclimatic indicators of environmental shifts from Bed I and Bed II times of the Olduvai Gorge, Tanzania. *Palaeogeogr Palaeoclimatol Palaeoecol.* **511**, 550–557 (2018).
9. Rivals, F. et al. Dietary traits of the ungulates from the HWK EE site at Olduvai Gorge (Tanzania): Diachronic changes and seasonality. *J. Hum. Evol.* **120**, 203–214 (2018).
10. Uno, K. T. et al. Large mammal diets and paleoecology across the Oldowan-Acheulean transition at Olduvai Gorge, Tanzania from stable isotope and tooth wear analyses. *J. Hum. Evol.* **120**, 76–91 (2018).
11. Negash, E. W. et al. Dietary trends in herbivores from Shungura Formation, southwestern Ethiopia. *PNAS* **117** (36), 21921–21927 (2020).
12. Semaw, S. et al. Co-occurrence of acheulian and oldowan artifacts with *Homo erectus* cranial fossils from Gona, Afar, Ethiopia. *Sci. Adv.* **6**, eaaw4694 (2020).
13. Mercader, J. et al. Earliest Olduvai hominins exploited unstable environments ~ 2 million years ago. *Nat. Commun.* **12**, 3 (2021).
14. Briatico, G., Bocherens, H., Bonnefille, R., Geraads, D. & Mussi, M. Isotopic insights into the Early Acheulean (1.95 Ma – 1.66 Ma) high-elevation paleoenvironments at Melka Kunture (Upper Awash Valley, Ethiopia). *Archaeol. Anthropol. Sci.* **15**, 184 (2023).
15. Briatico, G., Bocherens, H., Geraads, D., Melis, R. T. & Mussi, M. The Pleistocene high-elevation environments between 2.02 and 0.6 Ma at Melka Kunture (Upper Awash Valley, Ethiopia) based upon stable isotope analysis. *Sci. Rep.* **14**, 6619, 1–11 (2024).
16. Briatico, G., Mussi, M., Melis, R. T., Geraads, D. & Bocherens, H. Intra-tooth isotopic analysis shows seasonal variability in the high-elevation context of Melka Kunture (Upper Awash Valley, Ethiopia) during the Early Pleistocene. *Palaeogeogr Palaeoclimatol Palaeoecol*. **655**, 112555 (2024).
17. Domínguez-Rodrigo, M. Is the savanna hypothesis a dead concept for explaining the emergence of the earliest hominins? *Curr. Anthropol.* **55**, 59–81 (2014).
18. Su, D. F. & Haile-Selassie, Y. Mosaic habitats at Woranso-Mille (Ethiopia) during the Pliocene and implications for Australopithecus paleoecology and taxonomic diversity. *J. Hum. Evol.* **163**, 103076 (2022).
19. Negash, E. W. et al. Modern African ecosystems as landscape-scale analogues for reconstructing woody cover and early hominin environments. *J. Hum. Evol.* **197**, 103604 (2024).
20. Caley, T., Souron, A., Uno, K. T. & Macho, G. A. Climate and Human Evolution: Insights from Marine Records. *Annu. Rev. Mar. Sci.* **17**, 91–931 (2024).
21. Foister, T. I. F. et al. Quantifying heterogeneity of hominin environments in and out of Africa using herbivore dental traits. *Quat Sci. Rev.* **337**, 108791 (2024).
22. Raia, P. et al. Extinctions of *Homo* species coincided with increased vulnerability to climatic change. *One Earth*. **3**, 480–490 (2020).
23. Lupien et al. Abrupt climate change and its influences on hominin evolution during the early Pleistocene in the Turkana Basin, Kenya. *Quat. Sci. Rev.* 245, 106531 (2020).
24. Joordnes et al. An astronomically-tuned climate framework for hominins in the Turkana Basin. *Earth Planet. Sci. Lett.* **307**, 1–8 (2011).
25. Lüdecke et al. Persistent C_3 vegetation accompanied Plio-Pleistocene hominin evolution in the Malawi Rift (Chiwondo Beds, Malawi). *J. Hum. Evol.* **90**, 163–175 (2016).
26. Lüdecke et al. : Dietary versatility of Early Pleistocene hominins. *PNAS* **115** (52), 13330–13335 (2018).
27. Bonnefille, R. Evidence for a cooler and drier climate in the Ethiopian uplands towards 2.5 Myr ago. *Nature* **303**, 487–491 (1983).
28. Bonnefille, R., Melis, R. T. & Mussi, M. Variability in the mountain environment at melka kunture archaeological site, ethiopia, during the early pleistocene (~ 1.7 Ma) and the mid-pleistocene transition (0.9 – 0.6 Ma). In: (eds Gallotti, R. & Mussi, M.) The emergence of the acheulean in East Africa. Cham: Springer (2018).
29. Friis, I., Demissew, S. & Van Breugel, P. Atlas of the potential vegetation of Ethiopia. *Biologiske Skrifter*. **58**, 1–307 (2010).
30. Mairal, M. et al. Geographic barriers and Pleistocene climate change shaped patterns of genetic variation in the Eastern Afromontane biodiversity hotspot. *Sci. Rep.* **7**, 45749 (2017).
31. Nicholson, S. E. A review of climate dynamics and climate variability in Eastern Africa. In: Johnson, T.C., Odada, E.O. (Eds.), *The Limnology, Climatology and Paleoclimatology of the East African Lakes*. The International Decade for the East African Lakes (IDEAL). Gordon and Breach, Newark, NJ, 25–56 (1996).
32. Awulachew, S. B., McCartney, M., Steenhuis, T. S. & Ahmed, A. A. *A review of hydrology, sediment and water resource use in the Blue Nile Basin*. Working Paper 131. Colombo, Sri Lanka, International Water Management Institute (IWMI) (2008).

33. Lemann, T., Roth, T. & Zeleke, G. Impact of precipitation and temperature changes on hydrological responses of small-scale catchments in the Ethiopian Highlands. *HSJ* **62** (2), 270–282 (2017).
34. Seleshi, Y. & Zanke, U. Recent changes in rainfall and rainy days in Ethiopia. *Int. J. Climatol.* **24**, 973–983 (2004).
35. Segele, Z. T., Lamb, P. J. & Leslie, L. M. Seasonal-to-interannual of ethiopian/horn of africa monsoon. Part I: associations of wavelet-filtered large-scale atmospheric circulation and global sea surface temperature. *J. Clim.* **22**, 3396–3412 (2009).
36. Segele, Z. T., Richman, M. B., Leslie, L. M. & Lamb, P. J. Seasonal-to-interannual of ethiopian/horn of africa monsoon. Part II: statistical multimodel ensemble rainfall predictions. *J. Clim.* **28**, 3511–3536 (2015).
37. Beltrando, G. & Camberlin, P. Interannual variability of rainfall in the eastern Horn of Africa and indicators of atmospheric circulations. *Int. J. Climatol.* **13**, 533–546 (1993).
38. Haile, T. Causes and characters of drought in Ethiopia. *Ethiop. J. Agric. Sci.* **10** (1–2), 85–97 (1988).
39. Nicholson, S. & Kim, J. The relationship of the ENSO to African rainfall. *Int. J. Climatol.* **17**, 117–135 (1997).
40. Nicholls, N. What are the potential contributions of El Niño-southern oscillation research to early warning of potential acute food-deficit situations? In: (ed Glantz, M. H.) Workshop on Usable Science: Food Security, Early Warning and El Niño. 25–28 October, Budapest, Hungary. National Center for Atmospheric Research, Boulder, 169–177 (1993).
41. Seleshi, Y. & Demarée, G. R. Rainfall variability in the Ethiopian Eritrean highlands and its links with the southern oscillation index. *J. Biogeogr.* **22**, 945–952 (1995).
42. Hovers, E. et al. The expansion of the Acheulian to the Southeastern Ethiopian Highlands: Insights from the new early Pleistocene site-complex of Melka Wakena. *Quat Sci. Rev.* **253**, 106763 (2021).
43. Clark, J. D. & Kurashina, H. An analysis of earlier stone age bifaces from Gadeb (locality 8E), northern Bale highlands, Ethiopia. *S Afr. Archaeol. Bull.* **34**, 93–109 (1979).
44. Clark, J. D. & Kurashina, H. Hominid occupation of the east-central highlands of Ethiopia in the Plio-Pleistocene. *Nature* **282**, 33–39 (1979).
45. Williams, M. A. J., Williams, F. M., Gasse, F., Curtis, G. H. & Adamson, D. A. Plio-Pleistocene environments at Gadeb prehistoric site, Ethiopia. *Nature* **282**, 29–33 (1979).
46. Clark, J. D. & Transitions *Homo erectus* and the acheulian: the ethiopian sites of gadeb and the middle awash. *J. Hum. Evol.* **16**, 809–826 (1987).
47. de la Torre, I. The early stone age lithic assemblages of gadeb (Ethiopia) and the developed oldowan/early acheulean in East Africa. *J. Hum. Evol.* **60**, 768–812 (2011).
48. Fricke, H. C., Clyde, W. C. & O'Neil, J. R. Intra-tooth variations in $\delta^{18}O$ (PO_4) of mammalian tooth enamel as a record of seasonal variations in continental climate variables. *Geochim. Cosmochim. Acta*. **62** (11), 1839–1850 (1998).
49. Kohn, M. J., Schoeninger, M. J. & Valley, J. W. Variability in oxygen isotope compositions of herbivore teeth: reflections of seasonality or developmental physiology? *Chem. Geol.* **152** (1), 97–112 (1998).
50. Nelson, S. V. Paleoseasonality inferred from equid teeth and intra-tooth isotopic variability. *Palaeogeogr Palaeoclimatol Palaeoecol.* **222** (1–2), 122–144 (2005).
51. Balasse, M., Tresset, A. & Ambrose, S. Stable isotope evidence ($\delta^{13}C$, $\delta^{18}O$) for winter feeding on seaweed by Neolithic sheep of Scotland. *J. Zool.* **270** (1), 170–176 (2006).
52. Bernard, A. et al. Pleistocene seasonal temperature variations recorded in the $\delta^{18}O$ of *Bison priscus* teeth. *Earth Planet. Sci. Lett.* **283** (1–4), 133–143 (2009).
53. Cerling et al. Stable Carbon and Oxygen Isotopes in East African Mammals: Modern and Fossil. In: Werdelin, L. (Ed.), Cenozoic Mammals of Africa. Oakland (CA), 941–952 (2010).
54. Kwiecien et al. What we talk about when we talk about seasonality—A transdisciplinary review. *Earth-Sci. Rev.* **225**, 103843 (2022).
55. Green et al. How teeth record and attenuate seasonal signals. *J. Archaeol. Sci.* **175**, 106148 (2025).
56. Souron, A., Balasse, M. & Boisserie, J. R. Intra-tooth isotopic profiles of canines from extant *Hippopotamus amphibius* and late Pliocene hippopotamids (Shungura Formation, Ethiopia): insights into the seasonality of diet and climate. *Palaeogeogr Palaeoclimatol Palaeoecol.* **342–343**, 97–110 (2012).
57. Cerling, T. E. et al. Stable isotope ecology of the common hippopotamus. *J Zool* **276** (2), 204–212 (2008).
58. Harris, J. M., Cerling, T. E., Leakey, M. G. & Passey, B. H. Stable isotope ecology of fossil hippopotamids from the Lake Turkana Basin of East Africa. *J. Zool.* **275**, 323–331 (2008).
59. Boisserie, J. R. et al. Diets of modern and late Miocene hippopotamids: evidence from carbon isotope composition and microwear of tooth enamel. *Palaeogeogr Palaeoclimatol Palaeoecol.* **221**, 153–174 (2005).
60. Laws, R. M. Dentition and ageing of the hippopotamus. *Afr. J. Ecol.* **6** (1), 19–52 (1968).
61. Passey, B. H. et al. Inverse methods for estimating primary input signals from time-averaged isotope profiles. *Geochim. Cosmochim. Acta*. **69**, 4101–4116 (2005).
62. Uno, K. T. et al. Bomb-curve radiocarbon measurement of recent biologic tissues and applications to wildlife forensics and stable isotope (paleo)ecology. *PNAS* **110**, 29, 11736–11741 (2013).
63. Souron, A. et al. Variable enamel growth rates in hippopotamid canines: Implications for seasonality reconstructions using inverse modeling of intra-tooth isotope data. EGU General Assembly. Vienna, Austria, 14–19 April 2024, EGU24-22198 (2024).
64. Suga Progressive mineralization pattern of developing enamel during the maturation stage. *J. Dent. Res.* **61**, 1532–1542 (1982).
65. Trayler, R. B. & Kohn, M. J. Tooth enamel maturation reequilibrates oxygen isotope compositions and supports simple sampling methods. *Geochim. Cosmochim. Acta*. **198**, 32–47 (2017).
66. Green, D. R. et al. Quantitative reconstruction of seasonality from stable isotopes in teeth. *Geochim. Cosmochim. Acta*. **235**, 483–504 (2018).
67. Passey, B. H. & Cerling, T. E. Tooth enamel mineralization in ungulates: implications for recovering a primary isotopic time-series. *Geochim. Cosmochim. Acta*. **66**, 3225–3234 (2002).
68. Cerling, T. E. et al. Stable isotope ecology of the common hippopotamus. *J Zool* **276** (2), 204–212. (2008).
69. Cerling, T. E. & Harris, J. M. Carbon isotope fractionation between diet and bioapatite in ungulate mammals and implications for ecological and paleoecological studies. *Oecologia* **120**, 347–363 (1999).
70. Codron, J. et al. Taxonomic, anatomical, and spatio-temporal variations in the stable carbon and nitrogen isotopic compositions of plants from an African savanna. *J. Archaeol. Sci.* **32** (12), 1757–1772 (2005).
71. Rai, X. & Dixon, R. A. The differences between NAD-ME and NADP-ME Subtypes of C_4 Photosynthesis: more than Decarboxylating Enzymes. *Front. Plant. Sci.* **7**, 1525 (2016).
72. Briatico, G. Isotopic insights into mammalian diets and local vegetation cover during the Oldowan-Acheulean transition at Garba IV and Gombore I (Melka Kunture, Upper Awash Valley, Ethiopia). *Quat Int.* **722**, 109707 (2025).
73. Okonkwo, C., Demoz, B. & Gebremariam, S. Characteristics of lake chad level variability and links to enso, precipitation, and river discharge. *Sci. World J.* **45893**, 1–13 (2014).
74. Diakhaté, M. et al. Oceanic forcing on interannual variability of sahel heavy and moderate daily rainfall. *J. Hydrometeorol.* **20**, 397–410 (2024).
75. Hoppe, K. A., Stover, S. M., Pascoe, J. R. & Amundson, R. Tooth enamel biomineralization in extant horses: Implications for isotopic microsampling. *Palaeogeogr Palaeoclimatol Palaeoecol.* **206**, 355–365 (2004).
76. Levin, N. E., Cerling, T. E., Passey, B. H., Harris, J. M. & Ehleringer, J. R. A stable isotope aridity index for terrestrial environments. *PNAS* **103** (30), 11201–11205 (2006).

77. Pederzani, S. & Britton, K. Oxygen isotopes in bioarchaeology: principles and applications, challenges and opportunities. *Earth-Sci. Rev.* **188**, 77–107 (2019).
78. de Winter, N. J., Snoeck, C. & Claeys, P. Seasonal cyclicity in trace elements and stable isotopes of modern horse enamel. *PLoS ONE*. **11**, e0166678 (2016).
79. Tieszen, L. L., Senyimba, M. M., Imbamba, S. K. & Troughton, J. H. The Distribution of C_3 and C_4 Grasses and Carbon Isotope Discrimination along an Altitudinal and Moisture Gradient in Kenya. *Oecologia* **37**, 337–350 (1979).
80. Wooller, M. J., Swain, D. L., Street-Perrot, F. A., Mathai, S. & Agnew, A. D. Q. An altitudinal and stable carbon isotope survey of C_3 and C_4 graminoids on Mount Kenya. *East. Afr. Nat. Hist.* **90** (1), 69–85 (2001).
81. Hailu, H., Beldados, A. & Redae, E. B. Zooarchaeological study from the Early Stone Age site of Gadeb (~1.4 Ma), south-central Ethiopia. Conference abstract, 9th Biennial Conference of the Eastern African Association of Palaeoanthropologists and Palaeontologists, July 28th – August 1st, 2024. Addis Ababa, Ethiopia (2024).
82. Negash, E. W. & Barr, W. A. Relative abundance of grazing and browsing herbivores is not a direct reflection of vegetation structure: implications for hominin paleoenvironmental reconstruction. *J. Hum. Evol.* **122**, 103328 (2023).
83. Sokolowski, K. G., Codding, B. F., Du, A. & Faith, J. T. Do grazers equal grasslands? Strengthening paleoenvironmental inferences through analysis of present-day African mammals. *Palaeogeogr Palaeoclimatol Palaeoecol.* **629**, 111786 (2023).
84. Geraads, D. Fauna from the early Acheulean site of Gombore IB, Melka Kunture, Upper Awash, Ethiopia: systematics and paleoecology. *Quat Int.* **719**, 109672 (2025).
85. Martínez-Navarro, B. et al. The earliest Ethiopian wolf: implications for the species evolution and its future survival. *Comm. Biol.* **6**, 530 (2023).
86. Gonfiantini, R., Roche, M. A., Olivry, J. C., Fontes, J. C. & Zuppi, G. M. The altitude effect on the isotopic composition of tropical rains. *Chem. Geol.* **181**, 147–167 (2001).
87. Poage, M. A. & Chamberlain, C. P. Empirical relationships between elevation and the stable isotope composition of precipitation and surface waters: considerations for studies of paleoelevation change. *Am. J. Sci.* **301**, 1–15 (2001).
88. Lemma, B. et al. Spatial and temporal ^{2}H and ^{18}O isotope variation of contemporary precipitation in the Bale Mountains, Ethiopia. *Isot. Environ. Health Stud.* **56** (2), 1–14 (2020).
89. Wright, P. G. Thermoregulation in the Hippopotamus on land. *Afr. Zool.* **22** (3), 237–242 (1987).
90. Mussi, M. et al. Early *Homo erectus* lived at high altitudes and produced both Oldowan and Acheulean tools. *Science* **382**, 6671, 713–718 (2023).
91. Mussi, M. et al. A surge in obsidian exploitation more than 1.2 million years ago at Simbiro III (Melka Kunture, Upper Awash, Ethiopia). *Nat. Ecol. Evol.* **7**, 337–346 (2023).
92. Mussi, M. et al. Une vue d'ensemble sur Melka Kunture, grand complexe de sites pléistocènes dans la vallée supérieure de l'Awash (Ethiopie). *L'Anthropologie* **126**, 102999 (2022).
93. Mussi, M. et al. Melka Kunture (Alto Awash, Etiopía) entre 2.000.000 y 5.000 años. *Salduie* **23** (1), 1–11 (2023).
94. Mussi, M. et al. Melka Kunture, Ethiopia): a MSA site with archaic *Homo sapiens* remains revisited. *Quat Int.* **343**, 28–39 (2014).
95. Mussi, M., Altamura, F., Bonnefille, R., De Rita, D. & Melis, R. T. The environment of the Ethiopian highlands at the Mid Transition: Fauna, flora, and hominins in the 850–700 ka sequence at Gombore II (Melka Kunture). *Quat Sci. Rev.* **149**, 259–268 (2016).
96. Di Vincenzo, F. et al. The massive fossil humerus from the Oldowan horizon of Gombore I, Melka Kunture (Ethiopia, > 1.39 Ma). *Quat Sci. Rev.* **122**, 207–221 (2015).
97. Melis, R. T. & Mussi, M. The paleolandscape of Melka Kunture (Ethiopia) at the time of the earliest human peopling. *Palaeogeogr Palaeoclimatol Palaeoecol.* **684**, 113520 (2026).
98. Balasse, M., Ambrose, S. H., Smith, A. B. & Price, T. D. The seasonal mobility model for prehistoric herders in the south-western Cape of South Africa assessed by isotopic analysis of sheep tooth enamel. *J. Archaeol. Sci.* **29**, 917–932 (2003).

Acknowledgements

We thank the EHA for granting permission to sample the faunal dental remains and export the tooth enamel samples. G.B. is personally thankful to Sahleselasie Melaku and Adugna Debalike, as well as to other members of the EHA staff, for facilitating the research activities in many ways. This research made use of the Yale Analytical and Stable Isotope Center (YASIC) directed by Prof. Brad R. Erkkila (Yale University). The manuscript underwent an extensive review process, spanning four rounds of peer review from December 18, 2025, to June 23, 2026. In total, we addressed comments from nine reviewers, a substantial number considering the specificity of the research topic. Among the reviewers, a special thank you is due to Prof. Margaret J. Schoeninger for her supportive comments.

Author contributions

G.B., G.H. and E.H. conceived and designed the research paper. The faunal fossil remains were identified by B.M.-N., N.K. and H.H. Sampling and sample processing for isotopic analysis were carried out by G.B. E.H. and T.G. are the principal investigators of the project and are responsible for the project research objectives, administration and funding acquisition. A.A., A.R., E.M.N., and P.R.R. provided contextual information. G.B. wrote the paper with inputs from G.H. and E.H. All the authors commented, edited and approved the final version of the submitted manuscript.

Funding

The research activities at MW, including stable isotope analysis, are funded by the Fritz Thyssen Foundation (grant number: #10.21.1.07AA), awarded to E.H. and T.G. B.M-N. is funded by María de Maeztu Grant 2024 (CEX2024-01485-M by MICIU/AEI/https://doi.org/10.13039/501100011033) and Generalitat de Catalunya 2021SGR 01238 (AGAUR). This paper is part of the Lady Davis Postdoctoral Fellowship (2023–2025) awarded to G.B. at the Department of Prehistory, Institute of Archaeology of the Hebrew University of Jerusalem (Israel). G.B. was further funded by the INQUA (International Union for Quaternary Research) fellowship 2025. G.B. is currently supported by the project "POOL - Investigating cultural and biological scenarios of late Neanderthals and *Homo sapiens* in Poland" (FIS-2023-01196, CUP J53C24004280001), led by Prof. Andrea Picin and funded by the Italian Ministry of University and Research (D.D. MUR n. 23178 of 10/12/2024).

Declarations

Competing interests

Prof. Asfawossen Asrat is an Editor of Scientific Reports but was not involved in the editorial handling or peer review of this manuscript. The remaining authors declare no competing interests.

Additional information

Supplementary Information The online version contains supplementary material available at https://doi.org/10.1038/s41598-026-60484-z.

Correspondence and requests for materials should be addressed to G.B. or G.H.

Reprints and permissions information is available at www.nature.com/reprints.

Publisher's note Springer Nature remains neutral with regard to jurisdictional claims in published maps and institutional affiliations.